JOURNAL OF MATERIALS SCIENCE **35** (2000) 3113–3119

Layered polymer-kaolinite nanocomposites

J. E. GARDOLINSKI, L. C. M. CARRERA
CEPESQ, Research Center of Applied Chemistry, Department of Chemistry, Federal University of Paraná (UFPR), P.O. Box 19081, 81531-990 Curitiba, PR, Brazil

M. P. CANTÃO
Research and Development Central Laboratory, Agreement UFPR/COPEL, P.O. Box 19067, 81531-970 Curitiba, PR, Brazil

F. WYPYCH*
CEPESQ, Research Center of Applied Chemistry, Department of Chemistry, Federal University of Paraná (UFPR), P.O. Box 19081, 81531-990 Curitiba, PR, Brazil
E-mail: wypych@quimica.ufpr.br

Kaolinite (K) was reacted with liquid dimethyl sulfoxide (DMSO) producing $K(DMSO)_{0.4}$. Highly ordered polymer/kaolinite materials were obtained by displacement of DMSO molecules in the $K(DMSO)_{0.4}$ intercalate by polyethylene oxide (PEO) or bacterial polyhydroxybutyrate (PHB), both in the melt state at 130°C and 180°C, respectively. The hybrid nanocomposites obtained were characterized by powder X-ray diffractometry (PXRD), Fourier Transform Infrared spectrometry (FTIR) and thermal analysis (simultaneous TG/DSC). The obtained results are consistent with the total replacement of DMSO molecules by the macromolecular linear chains that lie flat building a monolayer of the polymer in the interlayer space of kaolinite. The stoichiometry of the compounds estimated from the TG/DSC measurements are: $K(DMSO)_{0.40\pm0.02}$, $K(PHB)_{0.82\pm0.02}$, $K(PEO)_{3.40\pm0.02}$.

1. Introduction

Kaolinite (K) is one of the most ubiquitous clay minerals in the earth, mostly found in soils, sediments and sedimentary rocks and is one of the most important raw materials for industrial uses. This mineral is a hydrated aluminum disilicate possessing the ideal composition $Al_2Si_2O_5(OH)_4$. Kaolinite is a 1 : 1 dioctahedral clay mineral composed of structurally asymmetric layers. One side of layer is gibbsite-like with aluminum atoms coordinated octahedrially with apical oxygen atoms and hydroxyls. The other side of the layer is constituted by a silicate layer structure, where the silicon atoms are coordinated tetrahedrially to oxygen [1]. Thus the kaolinite structure is composed basically of a single silica tetrahedral sheet joined to a single alumina octahedral sheet with the oxygen planes exposed on one side of a layer and hydroxyls on the other.

Some examples of kaolinite intercalation with small polar molecules such as dimethylsulfoxide (DMSO), n-methyl formamide (NMF), and hydrazine are frequently reported in the literature [2–5]. The intercalation of other compounds are also possible using the latter compounds as intercalated precursors using the so called "displacement method" [4, 6, 7].

Recently, many examples of polymer intercalated aluminosilicate have been reported [8–18]. Several methods were used to prepare these organic/inorganic hybrid materials involving the use of a clay suspension inside a polymer solution [8–11], the intercalation of entraining monomeric species followed by in-situ polymerization [13–18], by displacement of a previously formed intercalation complex [4, 6, 7] or mixing the clay directly with the liquid polymer melt to provide intercalation [12, 19–21]. In most of these examples of polymer/clay intercalation aluminosilicates of smectite group were used, where the hydration molecules of exchangeable ions of aluminosilicate are substituted by polymer molecules.

In spite of its great abundance, high crystallinity and high purity when compared with another mineral clays, only one example of kaolinite intercalation with organic polymers has been reported [19]. In this article was reported the intercalation of poly(ethylene glycol) (PEG) into the interlamellar spaces of kaolinite by displacing DMSO from a DMSO-kaolinite precursor mixed directly with a polymer melt. Powder X-ray diffraction (PXRD), FTIR spectroscopy and elemental analysis of intercalate revealed that intercalation could generate only partially DMSO substituted intercalates. In this example the polymer chains were arranged in flattened monolayers adopting preferentially a more relaxed trans conformation, causing an interlayer expansion of 0.4 nm.

From the above, nanostructured polymer/ceramic materials based on organoclays derived from smectites are a class of compounds where the intercalated

* Author to whom all correspondence should be addressed.

molecules are confined in a bidimensional space, acting only as a solvent to the exchangeable interlayer cations species. On the other hand, in kaolinite derivatives the intercalated molecules are directly bonded to the hydroxyls of the octahedric layer, providing an intimate molecular ensemble structure which can confer to these hybrid composites a set of unique and novel properties. In some cases synergistic effects can be envisaged when compared with only mechanically mixed polymer/clay compounds. Polymeric modified layered silicate nanocomposites (PLSN) are of considerable interest for designing high performance engineering materials with enhanced stiffness, strength, two dimensional stability, thermal and self-extinguishing characteristics [12].

Brazil is the third largest kaolin producer in the world with deposits in the Amazon basin greater than those already known in the rest of the world. Production capacity is being progressively increased and, in time, Brazil will probably emerge as the World's leading producer of high purity Kaolinite. In view of the success of nanocomposites based on smectites, this contribution reports the preparation of polymer/layered aluminosilicate, intercalates of polyethylene oxide and bacterial poly-β-hydroxybutyrate in kaolinite clay previously intercalated with DMSO. Monophasic materials (with a small contamination of residual kaolinite), were characterized by powder X-ray diffraction (PXRD), FTIR and thermal analysis (simultaneous TG/DSC).

2. Experimental

The kaolinite sample employed in this work (PP-0559) was supplied by Petrobrás Research Center (CENPES-Rio de Janeiro, Brazil) and it comes from the Amazon basin (Rio Capim deposit). It was received as finely divided pale-yellow powder of great purity, high crystallinity level and contaminated with minor concentrations of structural titanium and iron as determined by chemical analysis ($TiO_2 = 1.2 \pm 0.2$; $Fe_2O_3 = 0.7 \pm 0.1$) and electronic paramagnetic resonance (EPR) [22]. No crystalline contaminants were detected by powder X-ray diffraction (XRD). The kaolinite used to prepare the hybrid composites was used without further purification.

Polyethylene oxide, ($M = 10000$ g/mol) was purchased from Aldrich and bacterial poly-β-hydroxybutyrate ($M = 189.000$ g/mol) was obtained from Marlborough Biopolymers (Billinghan, UK), and purified by precipitation from N,N-dimethyformamide/diethylether.

Dimethylsulfoxide (DMSO), 1-methyl-2-pyrrolidone (NMP), N,N-dimethylformamide and diethylether were high-purity commercial Merck solvents used as received.

For powder x-ray diffraction analysis, the solid material was placed in the form of an oriented film in a neutral glass sample holder. The measurements were performed on a Rigaku diffractometer using Ni-filtered $Co_{K\alpha}$ radiation (λ : 0.17902 nm) with a dwell time of 1° min^{-1}. All measurements were taken using a generator voltage of 40 kV and a current of 20 mA. Powder of metallic silicon was added to the samples and used as internal standard. To remove undesirable radiation between the sample and the detector a homemade graphite monochromator was used (LORXI, Physics Department-UFPR).

The simultaneous TG-DSC measurements were performed on a Netzsch STA-409 EP series equipment under a static air atmosphere. Samples of about 20 mg were placed in alumina crucibles and heated between 30°C and 950°C at a rate of 5°C min^{-1}, using empty crucibles as reference.

FTIR spectra between 400 and 4000 cm^{-1} were obtained on a Bomem Michelson MB 100 FTIR spectrometer using 50 averaged scans at 2 cm^{-1} resolution. The solid samples were prepared as KBr pellets (ca. 3% by mass in KBr) while pure NMP was measured between two pellets of KBr.

Morphological study was carried out in a Philips XL30 scanning electron microscope operating at 30 kV. With this aim, nanocomposites and the pure kaolinite were suspended in water with manual stirring, deposited by casting directly in the copper sample holder and dried at room temperature for some hours. After that, they were sputtering coated with a thin gold film (nominal layer of 10 nm) to avoid charge buildups because of their low conductivity. No metallization effects over the morphology of these films have been observed.

2.1. Preparation of kaolinite-dimethylsulfoxide intercalate

The preparation of K-DMSO clay intercalate was conducted as follows: 9 g of kaolinite PP-0559 were mixed with 60×10^{-6} m^3 of DMSO and 5.5×10^{-6} m^3 of pure water and stirred to form a homogeneous suspension at 60°C. After 10 days the resulting material (K-DMSO) was separated by centrifugation at 4500 rpm for 3 minutes and dried in a drying oven at 50°C for 24 h to eliminate the excess of DMSO [2].

2.2. Preparation of kaolinite-polyethylene oxide intercalate

Immediately after drying and characterization, the K-DMSO intercalate was used as precursor to prepare polyethylene oxide intercalates conducted as follows: 2.5 g of PEO were mixed with 0.5 g of K-DMSO and ground in a agate vibrating mill (Fritsh-Analysette 3) for 30 minutes to obtain a finely divided powder. This reactional mixture was then transferred to a 50×10^{-6} m^3 reaction beaker and heated to fusion at 130°C for 4 days, under air. After that, the material was repeatedly washed with water, centrifuged and dried in a drying oven at 50°C for 48 h under air, to give a white powder.

2.3. Preparation of kaolinite-poly-3-hydroxy butyrate intercalate

K-DMSO intercalate was used as precursor to prepare poly-β-hydroxybutyrate intercalates conducted as follows: 0.8 g of PHB and 0.2 g of K-DMSO were mixed and ground in a agate vibrating mill (Fritsh-Analysette 3) for 30 minutes. This reactional mixture was then transferred to a 50×10^{-6} m^3 reaction beaker and heated to fusion at 180°C under air atmosphere

for 5 days. After the reaction, the intercalate, K-PHB was repeatedly washed with 1-methyl-2-pirrolydone and acetone and dried at 50°C for 24 h to give a slightly brown powder. In order to compare, the same polymer intercalate synthesis procedures were performed using only pure kaolinite. In this case no reaction was observed, which excludes the process of intercalation in absence of a precursor such as K-DMSO intercalate.

3. Results and discussion

3.1. Powder X-ray diffraction

The X-ray diffraction spectra of kaolinite (a), K-DMSO precursor (b), K-PEO (c) and K-PHB (d) are illustrated in Fig. 1. The interpretation of the X-ray reflections are summarized as follows: −K1 and K2; D1, D2 and D3; P1, P2 and P3; H1, H2, and H3 represent the first, second and third basal reflections of the raw kaolinite, K-DMSO, K-PEO and K-PHB intercalation compound, respectively.

Characteristic maxima of raw kaolinite were observed at $2\theta = 14.22^\circ$ (very intense, sharp and narrow) and $2\theta = 28.85^\circ$ (very intense, sharp and narrow). The peak at $2\theta = 14.22^\circ$ corresponds to the basal spacing of K (0.716 nm).

After intercalation, as expected, we can observe that the X-ray diffraction pattern of the original kaolinite modifies dramatically. The peak at $2\theta = 14.22^\circ$ in the original K, assigned as the first basal peak is greatly shifted in intercalates to small reflection angles due to expansion produced by the presence of intercalated DMSO or polymer chains. X-ray spectra for PEO and PHB showed that the characteristic diffraction peaks of the two pure macromolecular compounds do not appear in the X-ray diffraction pattern of kaolinite intercalates, which excludes the presence of any crystalline polymeric phase in the composites.

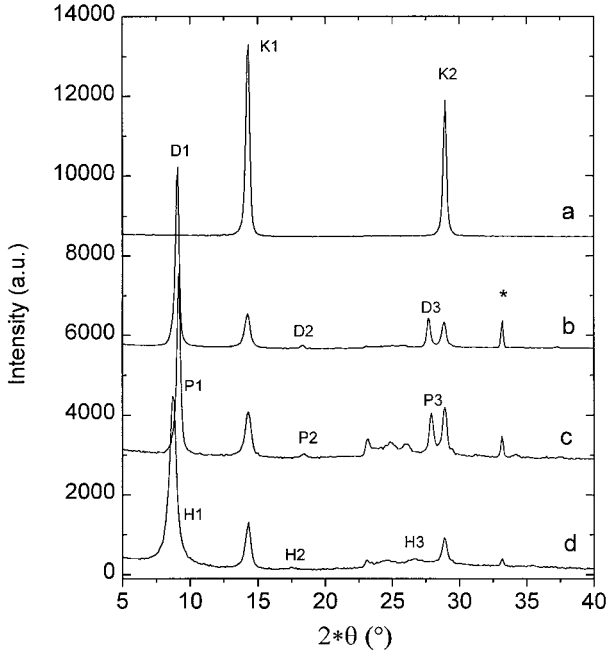

Figure 1 Powder X-ray diffraction of the raw kaolinite (a), K-DMSO (b), K-PEO (c) and K-PHB (d). The "*" represent the metallic silicon reflection, used as internal standard.

TABLE I Phase identification, intercalation ratio (IR), interlayer distances (d) and interlayer distances variation (Δd), related to raw kaolinite

Phase identification	IR (%)	d (nm)	Δd (nm)
K	—	0.716	—
K-DMSO	83.5	1.121	0.404
K-PEO	78.9	1.116	0.399
K-PHB	77.3	1.170	0.453

The interlayer spacing (d) and the interlayer expansion (Δd) with respect to pure kaolinite calculated from the Powder X-ray diffraction data (Fig. 1) are summarized in Table I. These results indicate that the confined polymer chains are arranged to give interlamellar flattened monolayer ensembles such as previously reported to oligomeric poly(ethylene glycol) [19].

The intercalation rates (IR) given as percentage (Table 1) were calculated from the powder X-ray data, as described in the Equation 1 [3].

$$\mathrm{IR} = \left\{ \frac{I_{i(001)}}{I_{k(001)} + I_{i(001)}} \right\} \cdot 100\% \qquad (1)$$

where $I_{i(001)}$ is the peak intensity observed for intercalate and $I_{k(001)}$ is the peak intensity observed for kaolinite.

These results show that displacement of DMSO in K-DMSO precursor by PEO and PHB was totally accomplished to give composites, regenerating an additional concentration of pure kaolinite. The IR drops from 83.5% in K-DMSO to 78.9% in K-PEO and 77.3% for K-PHB, respectively.

3.2. Thermal methods (TG/DSC)

Differential scanning calorimetry (DSC) and thermogravimetric analysis (TG) are two of the basic techniques for the characterization of organo-clay intercalates.

The K-DMSO intercalate shows a broad endothermic peak centered at 175°C, that corresponds to DMSO elimination [7]. The presence of this endothermic peak suggests that dimethylsulfoxide leaves the intercalate by simple volatilization without suffering any combustion reaction. An endothermic peak centered at 509°C corresponds to the dehydroxylation process of the kaolinite matrix. The same endothermic peak is observed at 529°C for the raw kaolinite. Considering that the residual kaolinite concentration was 16.5% and sample humidity 0.7%, the loss of organic matter from the intercalate was of 8.8% (dry weight basis) in agreement with the theoretical value of the same 8.8% (0, 4 DMSO for 1K). The total of residual mass measured by TG was of 79% (dry weight basis), which is very close to the theoretical value of 78.5% calculated from decomposition of kaolinite and intercalated dimethylsulfoxide.

Fig. 2 shows the typical TG/DSC curves for pure PEO (solid line) and intercalates K-PEO (dotted line).

The temperature values were determined as being the inflection points of the DSC curves. The TG/DSC curves obtained to K-PEO intercalate (dotted line)

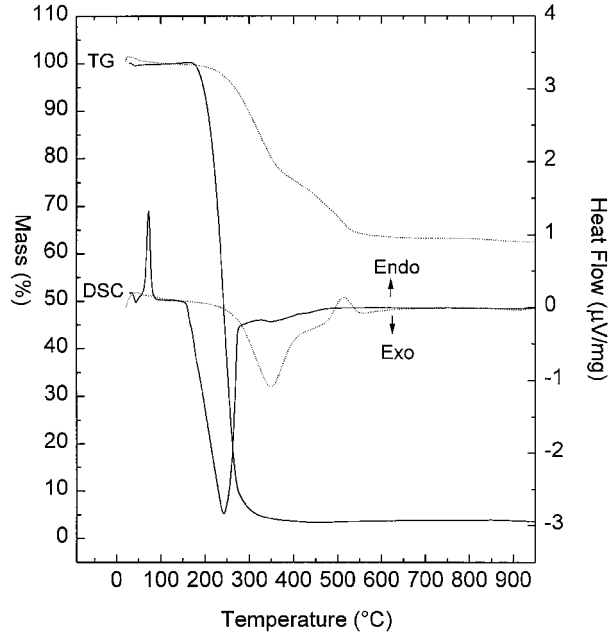

Figure 2 TG/DSC curve for pure PEO (solid line) and intercalates K-PEO (dotted line).

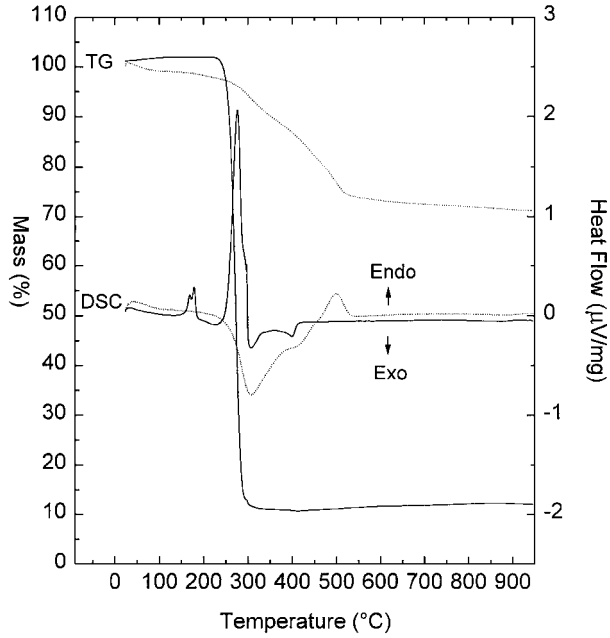

Figure 3 TG/DSC curve for pure PHB (solid line) and intercalates K-PHB (dotted line).

shows an exothermic peak centered at 349°C due to polymer thermolysis. In this intercalate, kaolinite decomposition produces an endothermic peak at 515°C. Considering that the concentration of kaolinite was 21.1% and sample humidity 0.9% the theoretical mass of PEO in the intercalate is 28.9% (dry weight basis) which is in good agreement with 28.8% obtained from thermogravimetric experiments (3.4 PEO for 1K related to $-OCH_2CH_3O-$ units). The total residual mass obtained from the TG curves for K-PEO intercalate was of 61.2% (dry weight basis), which is exactly the theoretical value of 61.2% calculated from decomposition of kaolinite and intercalated PEO.

It is interesting to note that in the DSC curve obtained for K-PEO, no peak was observed in the fusion region of PEO (around 73°C) (Fig. 2 —dotted line curve) which indicates that organo clay composite totally free of crystalline polymer was obtained, as was also suggested from our x-ray diffraction and scanning electron microscopic measurements.

Fig. 3 shows the typical TG/DSC curves for pure PHB (solid line) and intercalates K-PHB (dotted line). The temperature values were determined as being the onset points of the DSC curves.

The TG/DSC curves obtained from the K-PHB nanocomposite (dotted line) reveal a broad strong exothermic peak centered at 309°C followed by a shoulder at 408°C; both of them can be attributed to PHB thermal decomposition. In this intercalate, kaolinite decomposition produces an endothermic peak at 500°C. Considering that the concentration of kaolinite was 27.7% and sample humidity 1.9% the thermal weight loss until 450°C was 15.5% in full agreement with the theoretical calculated value of 15.6%. The total residual mass measured by TG for K-PHB intercalate was 72.7% (dry weight basis), identical to the theoretical value (72.7%), calculated from individual decomposition of kaolinite and intercalated PHB, confirming the results obtained from X-ray diffraction. The solid line shows the TG/DSC curve of pure PHB for comparison purposes. In this curve one can observe two endothermic peaks centered at 169 and 179°C attributed to the polymer fusion followed by an strong endothermic peak centered an 276°C with a shoulder at 294°C and one small exothermic peak at 400°C, attributed to the decomposition process of the pure polymer.

In neither curve were observed peaks at 175°C that can be attributed to the elimination of DMSO, showing that the presence of DMSO in the nanocomposites is excluded.

Table II summarizes the results obtained from the TG/DSC measurements. From these results the polymer stoichiometric quantities on intercalates could be calculated: $K(DMSO)_{0.40\pm0.02}$, $K(PEO)_{3.40\pm0.02}$ (related to $-OCH_2CH_2O-$ units), $K(PHB)_{0.82\pm0.02}$ (related to $-OCH(CH_3)CH_2CO-$ units) and considering the kaolinite formula as $Al_2Si_2O_5(OH)_4$) without any other contaminations.

The thermal analysis results show that the lamellar intercalation of PEO and PHB in kaolinite considerably alters their degradation patterns. The polymer confined chains reveal an increased thermal-oxidative stability and the decomposition thresholds are shifted from 220°C to about 243°C and 276°C for PEO and PHB respectively. Thus, intercalation provides an the efficient method to avoid direct contact of oxygen with the carbon chain preventing its degradation.

TABLE II Phase identification, humidity (%), organic matter (OM) (%), residual content (%)

Phase identification	Humidity (%)	OM (%)[a]	Residual (%)[a]
K	1.5	13.6	86.4
K-DMSO	0.7	8.8	79
K-PEO	0.9	28.9	61.2
K-PHB	1.9	15.5	72.7

[a]Related to the dry base.

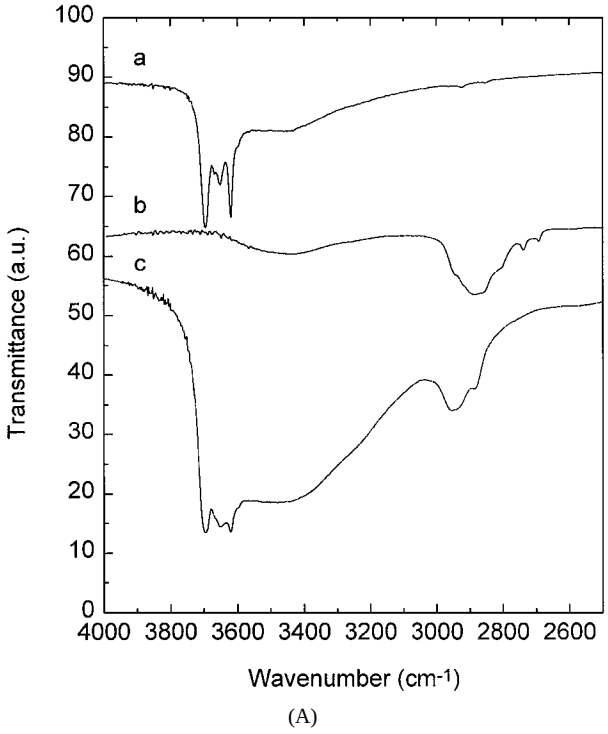

(A)

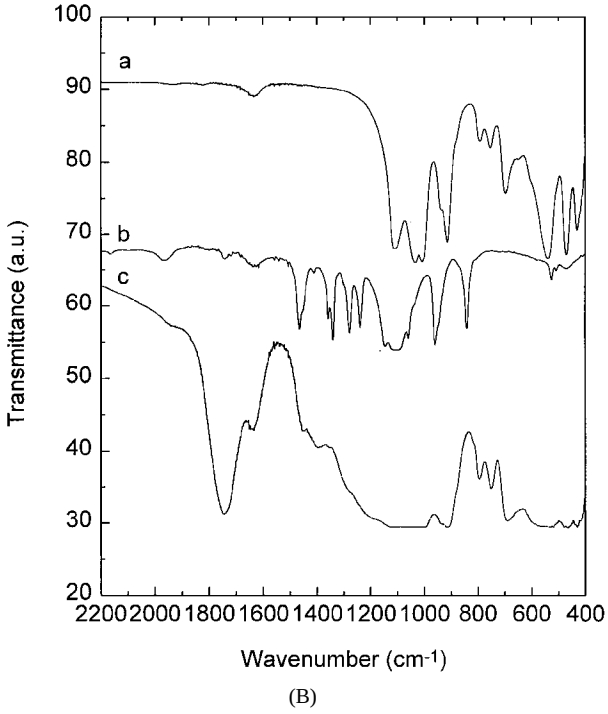

(B)

Figure 4 FTIR spectra of raw kaolinite (a), pure PEO (b) and K-PEO obtained on a KBr pellet over the 4000–2500 cm^{-1} region (A) and over the 2200–400 cm^{-1} region (B).

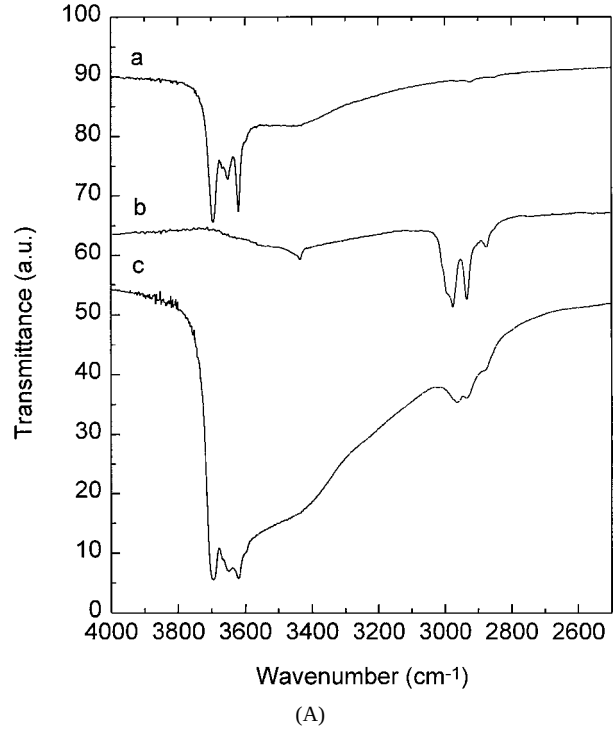

(A)

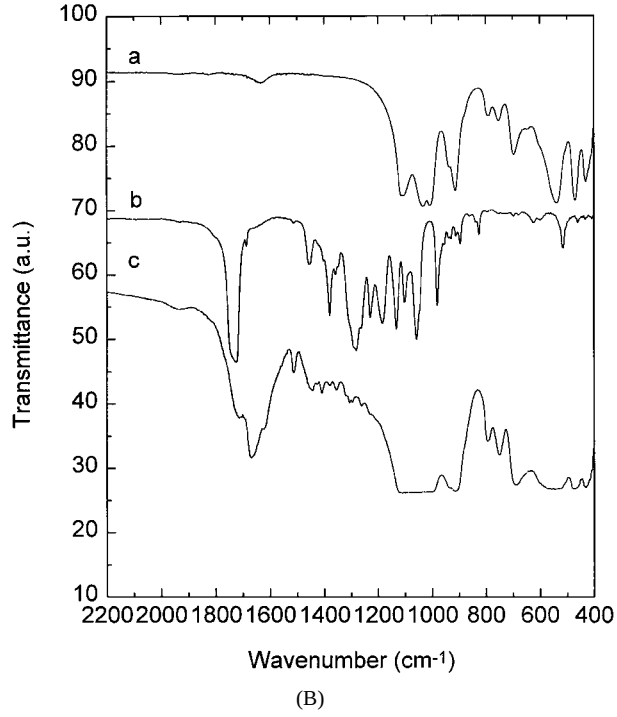

(B)

Figure 5 FTIR spectra of raw kaolinite (a), pure PHB (b) and K-PHB obtained on a KBr pellet over the 4000–2500 cm^{-1} region (A) and over the 2200–400 cm^{-1} region (B).

3.3. FTIR spectroscopy

The kaolinite and polymer intercalates were characterized by FTIR spectroscopy. Figs 4 and 5 shows the FTIR spectra of raw kaolinite (a), pure PEO (b) and K-PEO (Fig. 4) and raw kaolinite (a), pure PHB (b) and K-PHB (Fig. 5) obtained on a KBr pellet over the 4000–2500 cm^{-1} (A) and 2000–400 cm^{-1} region, respectively (B).

The presence of kaolinite in the nanocomposites can be evidenced by its absorption pattern in the 3500–3800 cm^{-1} range. The four bands observed in this region of spectrum (3694, 3668, 3650, 3619 cm^{-1}) can be assigned to the kaolin OH-stretching. The 3694, 3619 cm^{-1} doublet attributed for kaolin group in high crystalline ordered kaolinite [23] appears in K-PEO and K-PHB intercalates, as evidence that the intercalation process produces highly layered ordered composites. The presence of polymers in intercalates is evidenced by the characteristic C-H stretching bands of methylene groups over the 2600–3000 cm^{-1} region. It is interesting to note in K-PEO and K-PHB spectra the absence of the peaks observed in K-DMSO precursor, which confirms the total replacement of DMSO by the macromolecular species.

The C-H stretching frequencies of PEO and PHB in kaolinite intercalates appears slightly higher (10–70 cm^{-1}) than those observed in pure polymer. These results are consistent with those reported previously [19] indicating that PEO chains have more restricted conformation motion when confined in kaolinite lamellar space.

As can be seen the intercalation process, conducted in our case under air atmosphere, can induce the formation of slightly PEO and PHB carbonylated chains. The oxidative process occurring during intercalation is clearly evidenced by the absorption pattern in the 1800–1500 cm^{-1} range and seems to be more intense for PEO intercalates. Surprisingly, this feature of intercalation process conducted under air atmosphere was not observed by Tunney *et al*. [19], when working with the same intercalation conditions.

3.4. Morphological analysis

The morphology of pure kaolinite and K-PHB intercalate are illustrated in Fig. 6 (a and b), where scanning

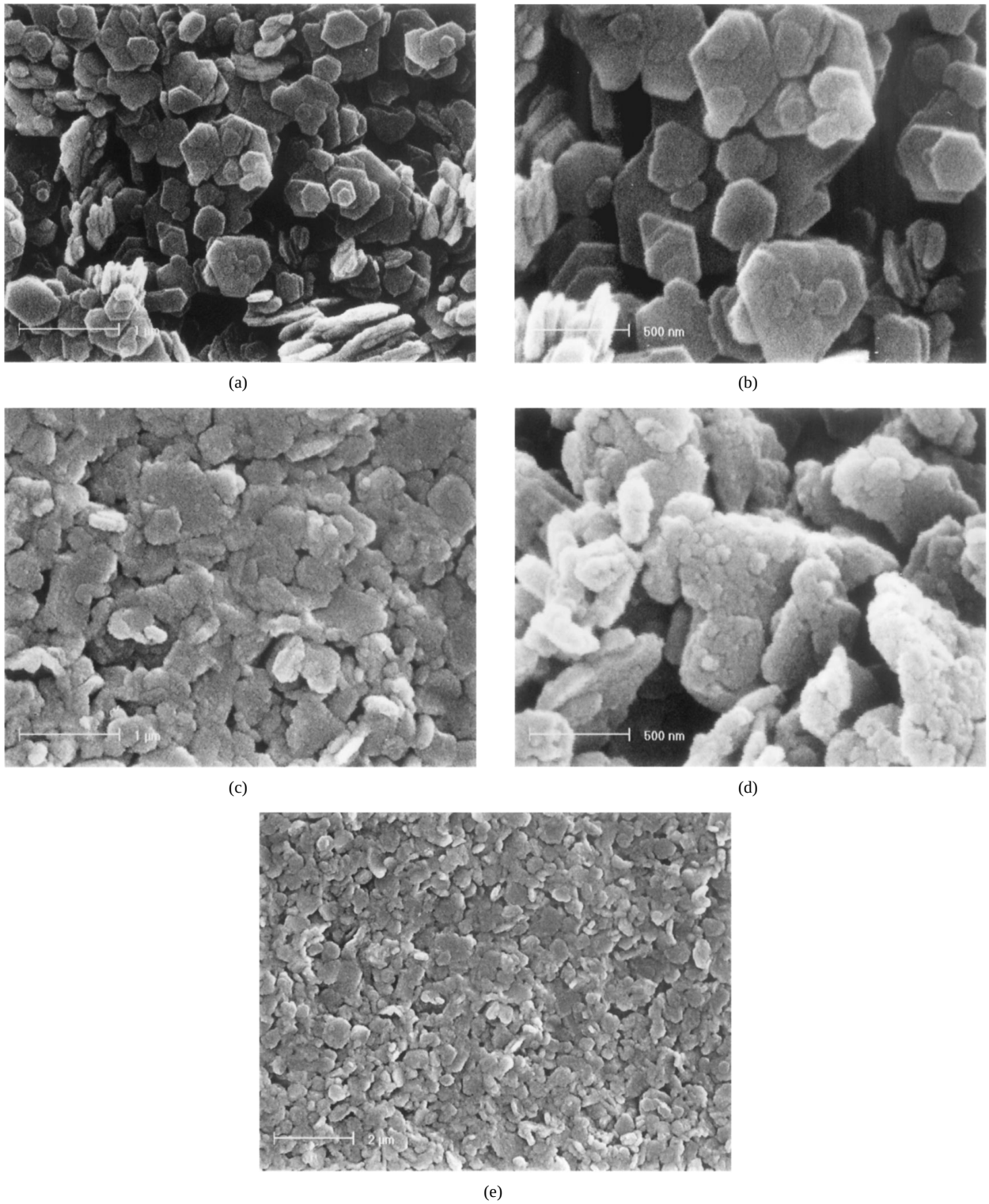

(a) (b) (c) (d) (e)

Figure 6 SEM measurements from raw kaolinite (a and b) and K-PHB intercalated phase (c to e).

electron micrographs with magnification varying from 25000× to 50000× were taken from cast film surfaces. For pure kaolinite a typical microstructure is shown in Fig. 6a (25000×). As can be seen, kaolinite is composed of highly perfect small platelets (0.2 to 2 μm) of ca. 80 nm thickness, showing morphology with well defined hexagonal edges and corner angles (120°). Scanning electron microscopy of K-PHB nanocomposite (6c to e) revealed significant morphological differences between pure kaolinite and polymer intercalates. K-PHB crystallites had varying degrees of imperfection, showing rounded edges and corners. In some cases the hexagonal pattern morphology has totally collapsed. The comparative microscopic analysis of K and K-PHB (Fig. 6b and d), also reveals that the intercalation process provokes a severe modification of crystallite surface. The surface degradation in K-PHB intercalates can be explained by the fact that lateral crystalline expansion during the thermal intercalation process causes the kaolinite to break the layers, which finally induces the crystallite disruption in several submicroscopic size crystallites. It is important to note that morphology of intercalates depends not only on intercalation expansion but can be highly affected by external factors such as mechanical agitation and washing of compounds during preparation and purification steps. In spite of this, when observed with lower magnification (Fig. 6e), it is clearly seen that K-PHB can form a very homogeneous and compact film. It suggests that PHB can act not only as the intercalate molecule, but also as an efficient composite binder. The observed apparent rounded areas on the SEM micrographs in the intercalated kaolinite can be related to sample preparation. Although an extensive washing procedure was applied to the samples, the apparent softening of edge definition can be the result of the polymer used to cover them. Similar results have been observed in K-PEO intercalates.

4. Conclusions

Polymer clay hybrid composites based on polyhydroxybutyrate (PHB) and polyethylene oxide (PEO)—kaolinite were successfully prepared by a simple fusion technique under air atmosphere conditions. This method has shown to be useful to prepare hybrid composites with intercalation index of 78.9% and 77.3% for PEO and PHB respectively. The polymer-clay intercalates have shown to be ordered arranged in flattened monolayers, such that the interlayer expansions determined by XRD were 0.399 nm and 0.453 nm for K-PEO and K-PHB respectively. The organokaolinite nanocomposites exhibit enhanced thermal stability as corroborated by TGA and DSC analysis. Investigations using scanning electron microscopy have demonstrated that intercalation processes provoke a severe degradation of kaolinite precursor morphology by a mechanism comprising initially of kaolinite interlayer expansion and surface fissure propagation. However, homogenous and compact polymer intercalate film could be obtained. This probable degradation can be also related to the sample preparation or measurement conditions. Nanomechanical properties studies of these nanocomposites are under way and will be the subject of a future publication.

Acknowledgements

The Physics Department at the Federal University of Paraná (UFPR) for the powder x-ray diffraction analysis and LAC-COPEL for the Scanning Electron Microscopic measurements.

References

1. E. AKIBA, H. HAYAKAWA, S. HAYASHI, R. MIYAWAKI, S. TOMURA, Y. SHIBASAKI, F. IZUMI, H. ASANO and T. KAMIYAMA, *Clays Clay Min.* **45** (1997) 781.
2. J. G. THOMPSON and C. CUFF, *ibid.* **33** (1985) 490.
3. P. J. R. UWINS, I. D. R. MACKINNON, J. G. THOMPSON and A. J. E. YAGO, *ibid.* **41** (1993) 707.
4. S. OLEJNIK, A. M. POSNER and J. P. QUIRK, *Clay Min.* **8** (1970) 421.
5. S. OLEJNIK, L. A. G. AYLMORE, A. M. POSNER and J. P. QUIRK, *J. Phys. Chem.* **72** (1968) 241.
6. Y. SUGAHARA, S. SATOKAWA, K. YOSHIOKA, K. KURODA and C. KATO, *Clays Clay Miner.* **37** (1989) 143.
7. F. WYPYCH, J. E. GARDOLINSKI and P. PERALTA-ZAMORA, *J. Colloid Interface Sci.* **211** (1999) 137.
8. P. ARANDA and E. RUIZ-HITZKY, *Chem. Mat.* **4** (1992) 1395.
9. V. MEHROTRA and E. P. GIANNELIS, *Solid State Commun.* **77** (1991) 155.
10. J. WU and M. M. LERNER, *Chem. Mat.* **5** (1993) 835.
11. E. RUIZ-HITZKY, P. ARANDA, B. CASAL and J. C. GALVÁN, *Adv. Mat.* **7** (1995) 180.
12. E. P. GIANNELIS, *ibid.* **8** (1996) 29.
13. Y. SUGAHARA, S. SATOKAWA, K. KURODA and C. KATO, *Clays Clay Miner.* **36** (1988) 343.
14. *Idem., ibid.* **38** (1990) 137.
15. E. P. GIANNELIS, *J. Met.* **44** (1992) 28.
16. P. B. MESSERSMITH and E. P. GIANNELIS, *Chem. Mat.* **6** (1994) 1719.
17. M. S. WANG and T. J. PINNAVAIA, *ibid.* **6** (1994) 468.
18. T. LAN and T. J. PINNAVAIA, *ibid.* **6** (1994) 2216.
19. J. J. TUNNEY and C. DETELLIER, *ibid.* **8** (1996) 927.
20. R. A. VAIA, H. ISHII and E. P. GIANNELIS, *ibid.* **5** (1993) 1694.
21. R. A. VAIA, S. VASUDEVAN, W. KRAWIEC, L. G. SCANLON and E. P. GIANNELIS, *Adv. Mat.* **7** (1995) 154.
22. Non published results.
23. Departamento Nacional de Produção Mineral—DNPM—Sumário Mineral Brasileiro, 1998. http://www.cprm-be.gov.br.
24. R. L. FROST and A. M. VASSALLO, *Clays Clay Min.* **44** (1996) 635.

Received 4 February
and accepted 15 December 1999